Crack growth simulation by BEM for SEN-specimens undergoing torsion or bending loading

R. Citarella[1], F.-G. Buchholz[2]

[1] Department of Mechanical Engineering, University of Salerno, via Ponte don Melillo 1, Fisciano (Salerno), ITALY, rcitarella@unisa.it
[2] Institute of Applied Mechanics, University of Paderborn, Paderborn, GERMANY

ABSTRACT. *In this paper the rather complex 3D fatigue crack growth behavior in 3PB-specimens or in cantilever beam specimens undergoing respectively bending or torsion loading, with inclined planes for the initial crack, is investigated by the aid of the BEM program BEASY. Mixed mode conditions along the crack edge are characterized. The stress intensity factors (SIFs) are determined using the crack opening displacement method (COD) and the crack growth direction is computed by the minimum strain energy density criterion. It will be shown that the computationally simulated results of fatigue crack growth in the Boundary Element (BE) model of the specimen are in good agreement with experimental findings for the development of the spatially twisted or twisted and warped crack faces in the real laboratory test-specimens. In particular, the comparisons with experimental findings are related to the evolving crack shape. The BEM results are also compared with FEM results, for which the SIFs are computed by the virtual crack closure integral (VCCI)-method and strain energy release rates (SERRs) and for the evolving 3D crack shape the* σ'_1 *criterion is adopted as fracture criterion. Consequently, also for these cases with a rather complex 3D crack growth behaviour, the functionality of the BEASY programme and the validity of the proposed 3D fracture criterion can be stated.*

INTRODUCTION

A number of fracture criteria for predicting the initiation and the direction of fatigue crack growth under mixed-mode I and II crack tip loading conditions are well established. But for the corresponding 3D case this can not be stated, because only a few 3D fracture criteria have been proposed so far and besides some theoretical and computational investigations there is only very limited experimental work available on which they could be based and proved. In this paper detailed results of two computational 3D fatigue crack growth simulations will be presented with reference to [1, 2]. The simulations are based on a Minimum Strain Energy Density criterion (in the following we will use the acronym MSED) [3] and on the Dual Boundary Element Method (DBEM) as implemented in the commercial BE-programme BEASY. The specimens under investigation are single edge notched (SEN) specimens with an inclined crack or notch plane and subject to three point

bending or torsion loading, respectively. In both cases the cracks initiate under general and variable mixed-mode loading conditions along the initial crack or notch front. In the case of three point bending the crack faces twist spatially until they finally intersect the free surface of the specimen opposite of the initial notch in a straight line perpendicular to the free side surfaces of the specimen. In the case of torsion loading the crack faces twist and warp spatially and finally intersect the free surface of the specimen opposite of the initial notch in a kind of S-shaped curve. The following investigation is focussed only on the complex 3D shape or geometry of the developing crack faces, because experimental values for crack growth rates comparisons are not available.

BE-MODEL OF THE SEN-SPECIMEN UNDER THREE POINT BENDING

The geometrical and material parameters of the 3PB-specimen (Fig. 1) are as follows: length L=260mm, 2Le=240mm, thickness t=20mm, width w=60mm, normalised initial crack length a/w=0.236 (for the experimental test the initial ratio a/w=1/3 is adopted but this is not detrimental to the numerical-experimental comparison), angle of the inclined plane of the initial crack or notch $\gamma = 45°$; Young's modulus E=70.656 N/mm^2, Poisson's ratio ν=0.34, threshold-value ΔK_{th}=174 N/mm$^{3/2}$ and fracture toughness K_{IC}=862 N/mm$^{3/2}$. The specimen is subject to a cyclic lateral force of initially F_{max}=2kN and the stress ratio of the cyclic loading is R=0.1.

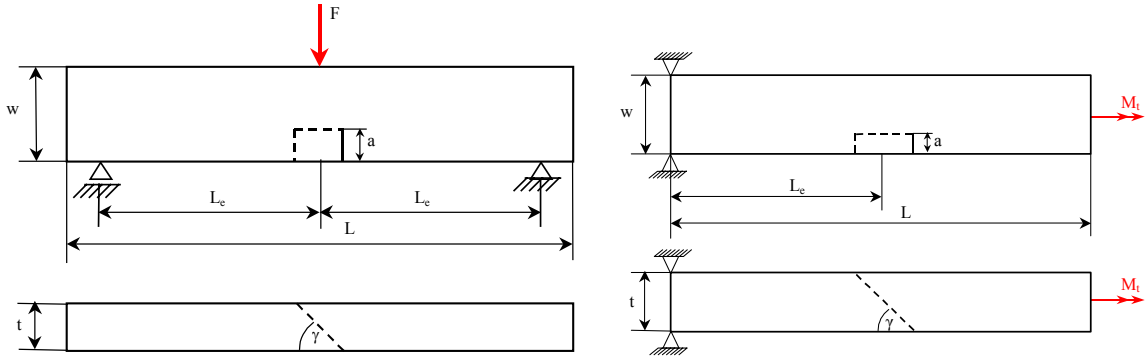

Figure 1. SEN-specimens with an inclined plane (γ =45°) of the initial crack or notch subject to three point bending (left) or to torsion loading (right).

In Figs. 2a-b the deformed 3D BE-models of the specimen are shown for the initial and incremented crack respectively, together with Von Mises stress highlight. Such models are assembled in the initial configuration from 243 *reduced quadratic* elements (the central node is missing) with 4110 degrees of freedoms. The crack and model remeshing during the propagation is automatically generated by the BEASY-programme. The number of elements has a moderate increase during the crack propagation due to the additional elements to form the new crack front. Adjacent to the initial crack plane a

moderate mesh refinement can be noticed. In order to calculate the Stress Intensity Factors (SIFs), which are required as input for the computational crack growth simulation, the Crack Opening Displacement (COD) technique is utilised by the BEASY-programme [4-5]. Discontinuous elements are used for the meshing of the crack surface and of the interface area separating the rough mesh from the fine mesh: this allow to easily refine the mesh where needed. The calculation of the strain energy density along the crack front is performed in order to define the direction of crack propagation, as provided by the MSED (with such criterion only the two basic fracture modes I, II are taken into account for the crack direction assessement).

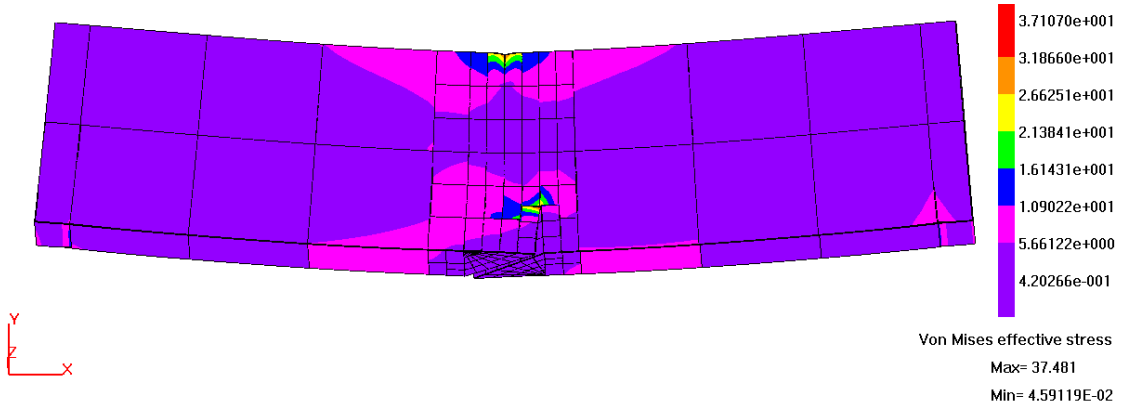

Figure 2a. Deformed BE-model of the 3PB-specimen (initial crack lenght a_i=14.1 mm).

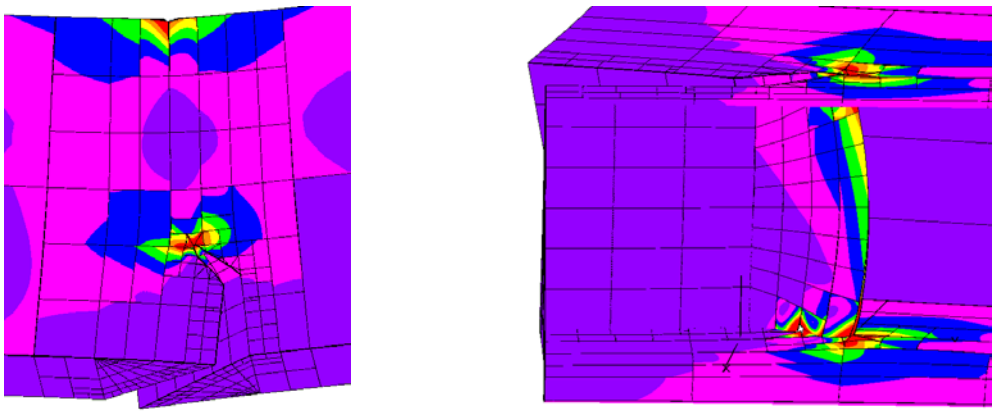

Figure 2b. External (left) and internal (right) view of the twisted crack after 4 steps of incremental crack growth (Δa_{max}=2 mm, displacement magnification factor DMF=250).

RESULTS FOR THE SEN-SPECIMEN UNDER THREE POINT BENDING

In Fig. 2b an opened crack and the spatially twisted crack faces can be seen. Furthermore a distinct anti-symmetric crack kinking can be noticed along the straight crack front of the inclined initial crack, with kink angles $\varphi_0>0$ for z/t>0.5 and $\varphi_0<0$ for z/t<0.5 (Fig. 3).

This is caused by the combination of the mode I and the anti-symmetric mode II loading conditions along the initial crack front (crack front 0) and which are given quantitatively, for the different crack propagation steps, in form of the $K_I(z/t)$ and $K_{II}(z/t)$-curves in Figs. 4-5 (SIFs along crack front are plotted). Due to the inclined plane of the initial crack also considerable mode III loading conditions are generated along the initial crack front and analysed in form of $K_{III}(z/t)$. The $K_{III}(z/t)$-curve (Fig. 6) is about constant except in the area close to the free surface.

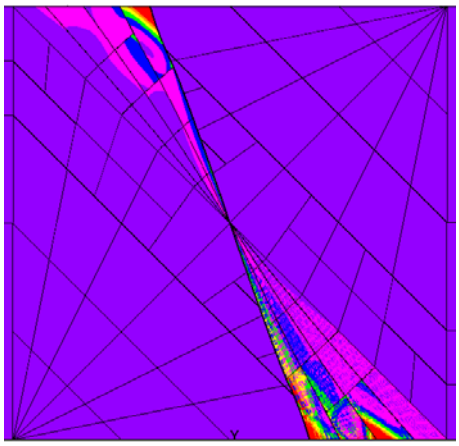

Figure 3. Crack kinking after 4 steps.

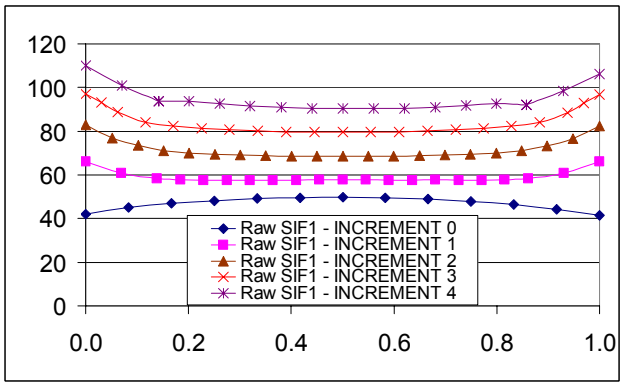

Figure. 4. K_I (MPa*mm$^{1/2}$) vs. z/t.

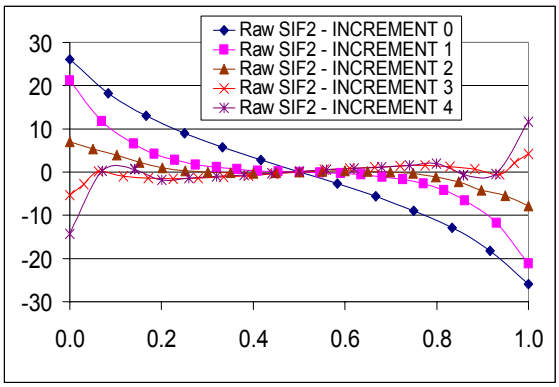

Figure.5. K_{II} (MPa*mm$^{1/2}$) vs. z/t.

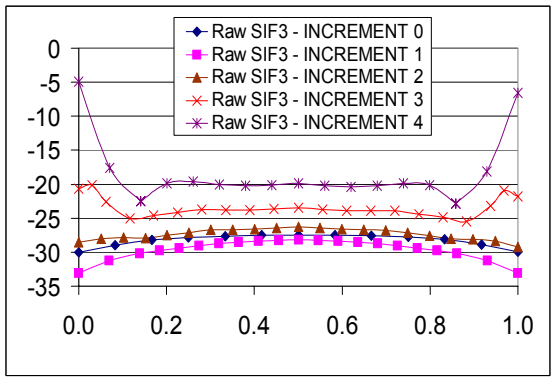

Figure.6. K_{III} (MPa*mm$^{1/2}$) vs. z/t.

After few crack increments the mode II loading conditions along the new crack front almost have disappeared (but for the zone close to the free surface). This obviously is due to the variable crack kinking with $\varphi_0(z/t)$ along the crack front, as a result of its considerable variable mixed mode I and II loading conditions and the correlated input to the MSED implemented in BEASY. The Figures 4-6 show about vanishing values for $K_{II}(z/t)$ and with some delay also for $K_{III}(z/t)$, but permanently rising values for $K_I(z/t)$. Their more and more curved and spatially twisted properties are illustrated by a view against the z-axis of the specimen (Fig. 2b) and against the y-axis (Fig. 3), respectively.

From Fig. 2b (view against x axis) a practically self-similar propagation of the mainly convex curved crack fronts can be noticed. The initial crack plane is inclined with an angle γ =45° and will end with an angle $\gamma \rightarrow$90° (Fig. 3) and only mode I loading conditions along the final crack fronts. In Fig. 7 an internal view of the BE-mesh of the final crack (crack front 4) and the corresponding experimentally obtained crack in a specimen from PMMA are shown.

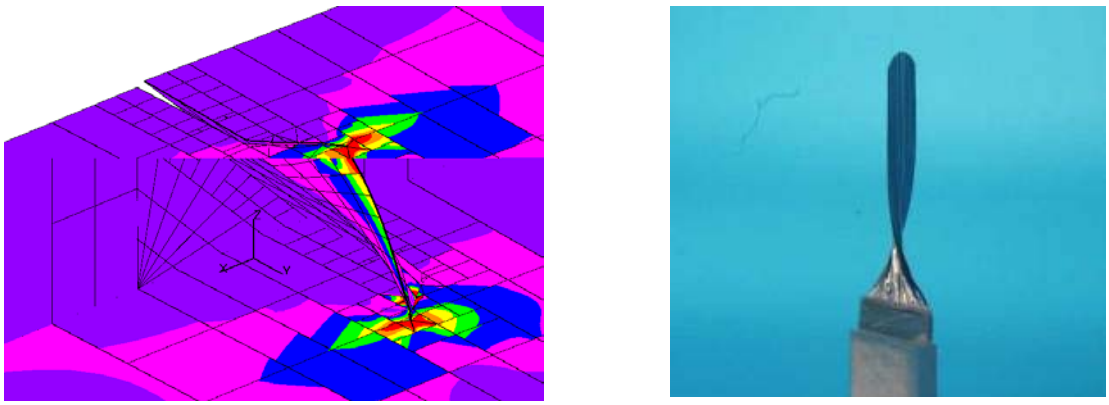

Fig. 7. Deformed plot of simulated final crack with highlight of Von Mises stress (left) and photo of a corresponding experimental crack in a 3PB-specimen from PMMA (right).

BE-MODEL OF THE SEN-SPECIMEN UNDER TORSION LOADING

The geometrical and material parameters of the SEN-specimen under torsion loading (Fig. 1b) are as follows: length L=2Le=160mm, thickness t=15mm, width w=20mm, normalised crack length a/w=0.25, angle of the inclined plane of the initial crack γ = 45deg.; Young's modulus E=2.1*10^5 N/mm^2 , Poisson's ratio ν=0.3, threshold-value ΔK_{th}=685 N/mm$^{3/2}$and fracture toughness K_{IC}=5091 N/mm$^{3/2}$. The specimen is subject to a cyclic torsion moment of initially M_{tmax}=200Nm which is acting around the x-axis of the specimen and the stress ratio of the cyclic loading is R=0.1. In Fig. 8a the deformed 3D BE-model of the specimen is shown for the initial crack (crack front 0). It is generated automatically by the BEASY-programme and is initially assembled from 343 *reduced quadratic* elements and 5295 degrees of freedoms. All further steps of computational fracture analysis and simulation are the same as described and discussed in conjunction with the preceding 3PB-problem.

RESULTS FOR THE SEN-SPECIMEN UNDER TORSION LOADING

In Figs. 8b-c the deformed BE-model of the twisted SEN-specimen is shown after few steps of simulated fatigue crack growth and clearly an opened crack and the spatially twisted and warped crack faces can be seen. A better impression of the global S-shape of the final crack one can get through Fig. 8d. A distinct anti-symmetric crack kinking can

be noticed along the straight crack front of the inclined initial crack, with kink angles $\varphi_0<0$ for $z/t>0.5$ and $\varphi_0>0$ for $z/t<0.5$. This obviously is caused by the combination of the mode I and the anti- symmetric mode II loading conditions along the initial crack front (crack front 0) and given quantitatively in form of the normalised $K_I(z/t)$ and $K_{II}(z/t)$-curves (Fig. 9a).

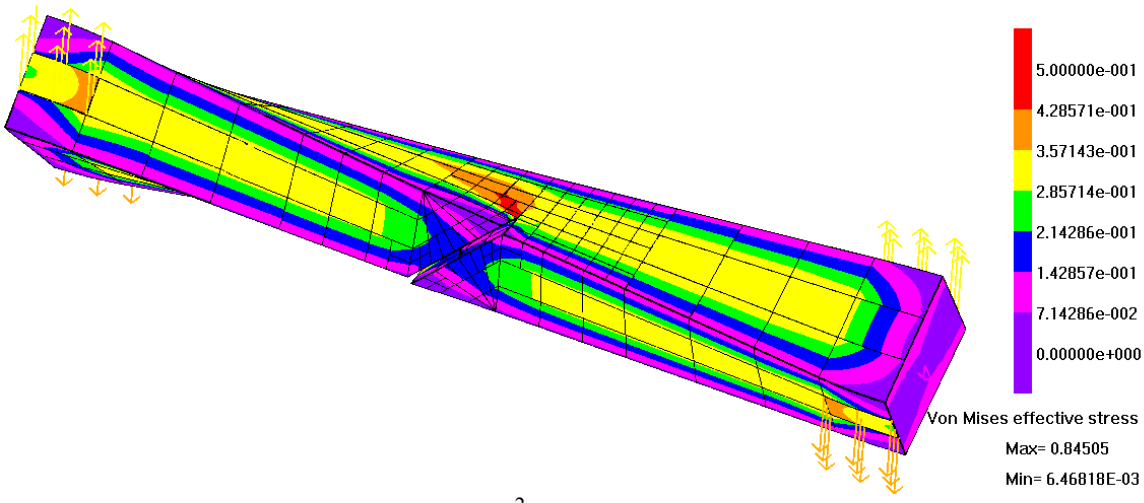

Figure 8a. Von Mises stress (kN/mm^2) on the deformed BE-model (DMF=50) of the twisted SEN-specimen with initial crack (a_i=5mm, γ =45°).

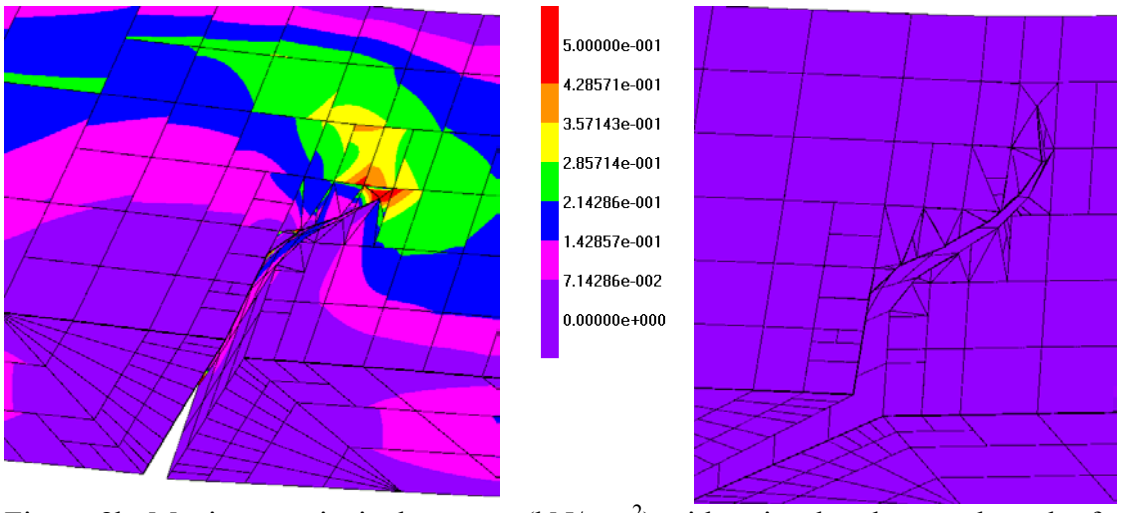

Figure 8b. Maximum principal stresses (kN/mm^2) with twisted and warped crack after 3 steps (left) and 6 steps (right) of crack growth (Δa_{max}=1.9 mm, DMF=10).

Due to the torsion loading of the specimen also mode III loading conditions are generated along the initial crack front and analysed in form of $K_{III}(z/t)$. The course of the $K_{III}(z/t)$-curve is about constant initially and its values are rather small, in particular compared to the predominant KI(z/t)-values, which are responsible for the pronounced

crack opening. The corresponding SIF-curves for the computationally simulated fatigue crack growth are given in Fig. 9b (crack fronts 0-3). The aforementioned graphs show about vanishing values for $K_{II}(z/t)$ and only small values for $K_{III}(z/t)$, compared with the permanently rising values for $K_I(z/t)$. Their more and more spatially curved properties are illustrated by a view against the x-axis (Fig. 8c) and against the y-axis (Fig. 8d). In Fig.10 the corresponding experimental findings for a test specimen from PMMA are presented (view against y axis).: by a digital photo a top view of the cracked specimen is shown which directly corresponds to the view against y axis of the simulated crack (Fig. 8d).

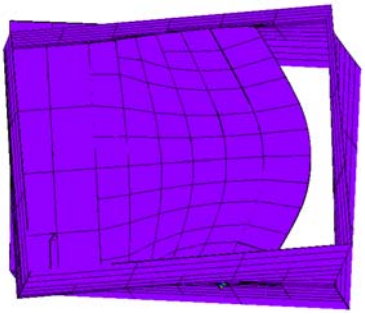

Figure 8c. Internal view of crack fronts as projected on yz plane.

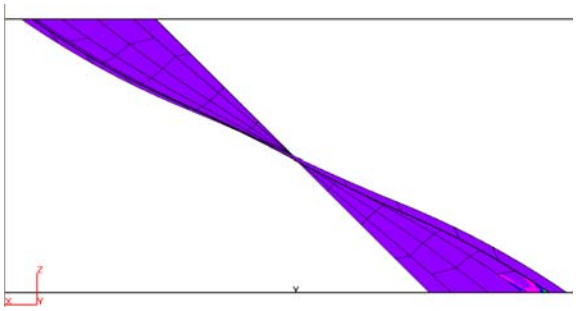

Figure 8d. Undeformed plot with highlight of S-shaped crack after 6 steps of crack growth.

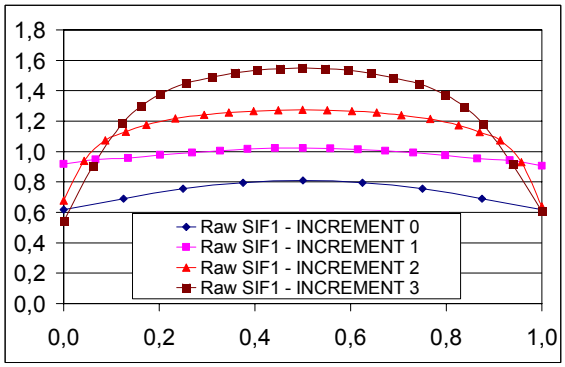

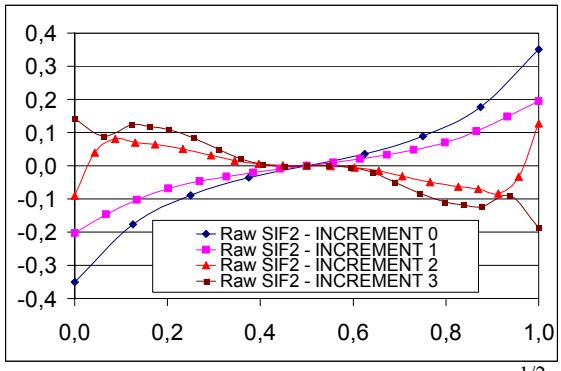

Figure 9a. K_I (left) and K_{II} (right) vs. z/t, along the crack front for each step (GPa*mm$^{1/2}$).

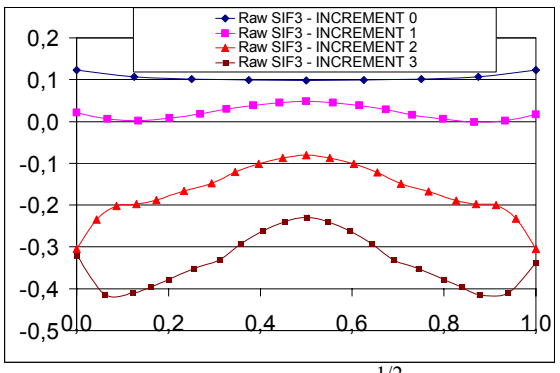

Figure 9b. K_{III} (GPa*mm$^{1/2}$) vs. z/t.

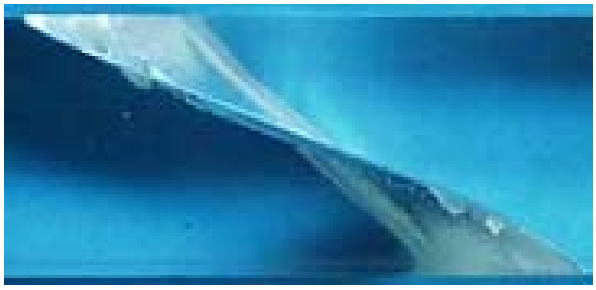

Figure 10. Cracked experimental specimen

CONCLUSIONS

The computational results are found to be in good qualitative agreement with experimental findings, which in both cases show a rather complex 3D crack growth behaviour. A satisfactory agreement can be stated also in comparison with FEM corresponding results [6-8]. Consequently, also for these cases the functionality of the BEASY-programme and the validity of the proposed 3D fracture criterion can be stated. Moreover it can be emphasized the reduced preprocessing times and run times involved: few minutes calculus were needed for the whole crack propagation process using a powerful PC (Pentium 3 GHz with 2GB of RAM).

REFERENCES

1. Buchholz F.-G., Just V., Richard H. A., Computational Simulation and Experimental Results on 3D Crack Growth in a 3PB-Specimen with an Inclined Crack Plane. In: Buchholz F.G., Richard H.A., Aliabadi M.H., editors, *Advances in Fracture Mechanics*, Trans Tech Publications, Zuerich, (1993), 2003, pp. 85-91.
2. Buchholz F.-G., Just V., Richard H.A., Computational Simulation and Experimental Results on 3D Crack Growth in a SEN-Specimen under Torsion Loading, In: Carpinteri A., Pook L.P., editors, CD-Rom Proceedings of Int. Conf. on Fatigue Crack Paths (FCP2003), Parma, (2003).
3. Sih, G.C., Cha, B.C.K., (1974), A fracture criterion for three-dimensional crack problems, *Journal of Engineering Fracture Mechanics* Vol. 6, pp. 699-732.
4. Calì C., Citarella R., Perrella M., Three-dimensional crack growth: numerical evaluations and experimental tests, *Biaxial/Multiaxial Fatigue and Fracture*, ESIS Publication 31, 2003, Ed. Elsevier, pp. 341-360.
5. Citarella R., Perrella M., (2005), Multiple surface crack propagation: numerical simulations and experimental tests, *Fatigue and Fracture of Engineering Material and Structures* Vol. 28, pp. 135-148.
6. Buchholz F.-G., Richard H.A., Comparison of Computational Crack Path Predictions with Experimental Findings for SEN-Specimens Under Different Loadings, In: *Computational Mechanics,* (Eds. Z. H. Yao et al), CD-ROM Proc. of the 6th World Congress of Computational Mechanics (WCCM VI) in conjunction with APCOM'04, September 2004, Beijing, China, Tsinghua University Press & Springer-Verlag, 2004.
7. Richard H.A., Buchholz F.-G., Kullmer G., Schöllmann M., (2003), 2D- and 3D-Mixed Mode Fracture Criteria, *Key Engineering Materials* Vols. 251-252, pp. 251-260.
8. Buchholz F.-G., Chergui A., Richard H.A., (2004), *Fracture Analyses and Experimental Results on Crack Growth Under General Mixed Mode Loading Conditions.* Engng Fract. Mech. Vol. 71, Issue 4-6, (special issue), pp. 455-468.